Supplementary Information

Probing the freezing chemistry of singly levitated aqueous trifluoroacetic acid droplets in a cryogenically cooled simulation chamber relevant to Earth's upper troposphere

Koushik Mondal[a], Souvick Biswas[a], Nils Melbourne[a], Rui Sun[a*], Ralf I. Kaiser[a*]

[a] Department of Chemistry, University of Hawai'i at Manoa, Honolulu, Hawaii 96822, United States

* Corresponding author. E-mail: ruisun@hawaii.edu; ralfk@hawaii.edu

Table of contents:

S1. Experimental details:

S1.1 Sample preparation: 99.99% Pure trifluoroacetic acid (TFA) was purchased from Sigma Aldrich and diluted in Millipore water (Thermo Fischer) in different weights to prepare different weight-by-weight (w/w) TFA solutions. The mole ratio of the substituent in the solution and the molarity are given below in Table S1.

Table S1: Different types of TFA solutions prepared and their respective molarity with molar ratio

w/w %	**Mole ratio** (TFA: Water)	**Molarity**
80%	2:1	11.49 (M)
10%	1:62	0.85 (M)
7.5%	1:84	0.60 (M)
5%	1:128	0.35 (M)
2.5%	1:236	0.23 (M)
1%	1:623	0.08 (M)

S1.2 Surface-free levitator set up in a cryogenically cooled process chamber to understand droplet freezing chemistry in upper troposphere

S1.2.1. Ultrasonic levitator apparatus: In the acoustic levitator apparatus utilized in this experiment, ultrasonic sound waves at a frequency of 58 kHz are generated by a piezoelectric transducer and reflected off a concave plate positioned vertically upwards, thereby creating a standing wave. These sound waves generate acoustic radiation pressure, enabling a liquid droplet or a small solid particle to levitate just below one of the pressure minima of the standing wave. The distance between the transducer and reflector is calibrated to 2.5 times the wavelength of the sound wave (approximately 14.8 mm), resulting in a total of five pressure nodes. However, only the second and third pressure nodes above the ultrasonic transducer are effective for levitation. The maximum diameter of droplets or particles that can be stably levitated in this apparatus is around 3 mm, while the minimum size can be as small as 15 μm. In this setup, water droplets positioned in the pressure node take on an oblate spheroidal shape due to the acoustic radiation pressure, and their volumes are calculated accordingly.

S1.2.2 Cryogenically cooled process chamber and sampling system: The levitator assembly is housed within a pressure-compatible process chamber, approximately 15 liters in volume, constructed from stainless steel. This design allows for levitation in either inert or highly reactive gases to facilitate the investigation of chemical reactions. The process chamber is equipped with spectroscopic tools (FTIR, Raman) and visualization equipment (high-speed optical and infrared cameras) to monitor any significant chemical or physical changes in the levitated samples. A custom cylindrical cooling jacket, filled with liquid nitrogen, is inserted from the top, and positioned between the chamber wall and the levitator unit to cool the internal environment. The cooling jacket features customized cuts to accommodate all spectroscopic and camera probes and is connected to a liquid nitrogen dewar located externally. Additionally, the process chamber is well insulated to enhance the cooling efficiency. During the experiments, the chamber was filled with nitrogen gas (Matheson, Research Purity 99.9999%) at a temperature of 293 K and a total pressure of 760 Torr.

S1.3 Key spectroscopic and optical techniques used:

In our experiments, Raman spectroscopy serves as the primary technique for investigating the freezing dynamics of TFA-doped water droplets. FTIR spectroscopy is also employed to detect gas phase constituents. The visual changes in the droplets are primarily monitored using a high-speed optical camera.

S1.3.1 Raman spectroscopy: In the Raman spectrometer, vibrational transitions are excited by a 532 nm line from a diode-pumped, Q-switched Nd:YAG laser (CrystaLaser, model QL532-1W0), which has a beam diameter of 0.35 mm and a divergence angle of 3.8 mR. The laser outputs an average power of approximately 200 mW with a pulse width of 13.5 ns, operating at a repetition rate of 1 kHz. The laser beam is introduced into the chamber through an antireflection-coated window, followed by a mirror (Edmund Optics, model NT45-991, >99% reflectance) and a dichroic beam splitter (Semrock, RazorEdge, model LPD01-532RU-25 × 36 × 2.0). A plano-convex lens with a focal length of 60 mm focuses the laser beam onto the sample, creating a spot with a diameter (1/e2) of approximately 20 μm. The Raman-shifted photons, backscattered from the droplet, pass through an ultra-steep long-pass edge filter (Semrock, model LP03-532RE-25) to eliminate elastically scattered 532 nm laser light. The resultant backscattered photons are then focused by a 50 mm f/1.8 camera lens (Nikon, Nikkor 2137) into a HoloSpec f/1.8 holographic imaging spectrograph (Kaiser Optical Systems, model 2004500-501 and Holoplex HPG-532) equipped with a PI-Max 2 ICCD camera (Princeton Instruments) through a 100 μm slit. The CCD detector consists of 1024 × 256 pixels, each with a spatial resolution of 26 μm. Spectra are collected over Raman-shift ranges of 200-2450 cm^{-1} and 2400-4000 cm^{-1} simultaneously, achieved by dispersing the total signal using two overlaid holographic transmission gratings. The resolution of the Raman spectrometer is 9 cm^{-1}. Both the excitation laser and the detector operate at a 1 kHz repetition rate, synchronized via a pulse generator, Quantum Composer Plus, model-9518. To isolate the Raman scattering signal, the pulse width for the ICCD detector is typically set around 50 ns, with accumulation times for each spectral trace ranging from 5 to 100 seconds. For the experiments presented, a typical gate delay of 480-500 ns was employed, with gates per exposure fixed at 1000 shots. The Raman spectrometer was calibrated by recording Raman spectra for levitating droplets of cyclohexane (C_6H_{12}), toluene ($C_6H_5CH_3$), and acetonitrile (CH_3CN).

The recorded Raman spectral features further processed by correcting baseline and deconvoluting with multi peak fitting. In most of our cases the deconvoluted peak area or peak heights are compared with the progress of the freezing. In order to extract kinetics information in the form of rate constant these plots constituted by the ratio of the deconvoluted peak areas or heights with respect to time are fitted by either by firs order exponentially increase or decrease factor respectively as

$Y= Y_0 + \exp(kx)$ and $Y= Y_0 + \exp(-kx)$

Where Y represent the ratio of peak areas or heights Y_0 is the initial ratio of area or peak height for a particular set, k is the rate constant in $second^{-1}$ (s^{-1}) obtained from the fitting and x is the time in second.

S1.3.2 FTIR spectroscopy: The FTIR absorbance spectra were recorded with a spectral resolution of 1 cm^{-1} across the full width of the process chamber, with an effective path length of 53.35 cm. The FTIR spectrometer system operates in a vacuum and combines a VERTEX 70v spectrometer (Bruker) with two stages of copper mirror optics and a liquid nitrogen-cooled MCT-B (mercury cadmium telluride, wide band, D315/B) detector.

S1.3.3 Optical and infrared movies and snapshots: To capture visuals of the freezing process, a Phantom Miro 3a10 camera, operating at a repetition rate of up to 1 kHz, was aligned with the levitated sample via an optical viewport. The temperature measured by the silicon diode sensor reflects the gaseous atmosphere inside the chamber and does not accurately represent the temperature of the levitated aqueous droplets. Therefore, a high-speed infrared camera (FLIR A6703sc) was utilized at a repetition rate ranging from 10 to 250 Hz to monitor temperature changes during the freezing of levitated water droplets into ice. The observable levitating samples were selected within the region of interest (ROI) of the camera for precise temperature readings, with the mean temperature in the selected ROI being considered. In the observed freezing event (Figure 2b), a typical repetition rate of 40 Hz was used, synchronized with the high-speed optical camera via a pulse generator (Quantum Composer Plus, model-9518). Notably, the temperature of the sample at the second pressure node was found to be closest to that of the surrounding atmosphere (as measured by the silicon diode temperature sensor) compared to other pressure nodes.

Table S2a: Raman spectral assignment of 80% and 10 % TFA solution at room temperature with relative intensity with respect to the most intense band of each spectrum

80% TFA solution (water:TFA=1:2)				10% TFA solution (water:TFA=62:1)			
Band number	Frequency	Assignment	Relative intensity	Band number	Frequency	Assignment	Relative intensity
ν_1^t	3466	O—H stretching TFA	15.29	ν_1	3405	O—H double donor single acceptor tetrahedral environment	100
ν_2^t	2959	O—H stretching of TFA dimer	3.64	ν_2	3224	O—H double donor double acceptor tetrahedral environment	79.50
ν_3^t	1771	C=O stretching TFA	14.38	ν_3	3035	O—H bending overtone water	6.47

ν_4^t	1461	C—O deformation TFA	12.99	ν_4	1768	C=O stretching TFA	2.60
ν_5^t	1213	C—F stretch out of phase TFA	6.60	ν_5	1676	C—O stretching TFA ion	2.29
ν_6^t	1170	C—F stretching TFA	8.56	ν_6	1622	O—H bending of water	0.80
ν_7^t	814	C—C stretch TFA	100	ν_7	1444	CO stretch TFA ion	25.76
ν_8^t	713	CO_2 deformation TFA	5.36	ν_8	1201	C—F stretch out of phase TFA ion	6.82
ν_9^t	599	CF_3 deform in phase TFA	23.92	ν_9	1154	C—F stretch in phase TFA ion	2.89
ν_{10}^t	520	CF_3 deform out of phase TFA	3.37	ν_{10}	846	C—C stretch TFA ion	9.61
ν_{11}^t	434	CF_3 rocking TFA	30.19	ν_{11}	818	C—C stretch TFA	20.54
ν_{12}^t	406	CF_3 rocking TFA	45.09	ν_{12}	724	CO_2 deformation TFA ion	5.62
ν_{13}^t	262	CF_3 twisting TFA	10.51	ν_{13}	599	CF_3 deform in phase TFA ion	9.9
				ν_{14}	521	CF_3 deform out of phase TFA ion	1.50
				ν_{15}	431	CF_3 rocking TFA ion	10.88

				ν_{16}	409	CF_3 rocking TFA	13.25

Table S2b: Raman spectral assignment of 10% TFA solution at room temperature and freezing temperature

10% TFA solution freezing temperature (262K)			10% TFA solution at room temperature		
Band number	Frequency	Assignment	Band number	Frequency	Assignment
ν^{I}_{1}	3351	O—H double donor single acceptor hexagonal environment	ν_1	3405	O—H double donor single acceptor tetrahedral environment
ν^{I}_{2}	3144	O—H double donor double acceptor hexagonal environment	ν_2	3224	O—H double donor double acceptor tetrahedral environment
ν^{I}_{3}	3134	O—H bending overtone water	ν_3	3035	O—H bending overtone water
ν^{I}_{4}	1624	O—H bending of water	ν_4	1768	C=O stretching TFA
ν^{I}_{5}	1444	CO stretch TFA ion	ν_5	1676	C—O stretching TFA ion
ν^{I}_{6}	1200	C—F stretch out of phase TFA ion	ν_6	1622	O—H bending of water

ν^{I}_{7}	1153	C—F stretch in phase TFA ion	ν_7	1444	CO stretch TFA ion
ν^{I}_{8}	1034	H bonding interaction with C-F	ν_8	1201	C—F stretch out of phase TFA ion
ν^{I}_{9}	844	C—C stretch TFA ion	ν_9	1154	C—F stretch in phase TFA ion
ν^{I}_{10}	820	C—C stretch TFA solid (most intense)	ν_{10}	846	C—C stretch TFA ion
ν^{I}_{11}	725	CO_2 deformation TFA ion	ν_{11}	818	C—C stretch TFA
ν^{I}_{12}	601	CF_3 deform in phase TFA solid	ν_{12}	724	CO_2 deformation TFA ion
ν^{I}_{13}	521	CF_3 deform out of phase TFA ion	ν_{13}	599	CF_3 deform in phase TFA ion
ν^{I}_{14}	435	CF_3 rocking TFA solid	ν_{14}	521	CF_3 deform out of phase TFA ion
ν^{I}_{15}	412	CF_3 rocking TFA solid	ν_{15}	431	CF_3 rocking TFA ion
ν^{I}_{16}	287	Liberational mode of ice	ν_{16}	409	CF_3 rocking TFA
ν^{I}_{16}	265	CF_3 twisting			

Figure S1: FTIR spectrum of pure TFA vapour at room temperature formed from the levitated droplet of pure TFA

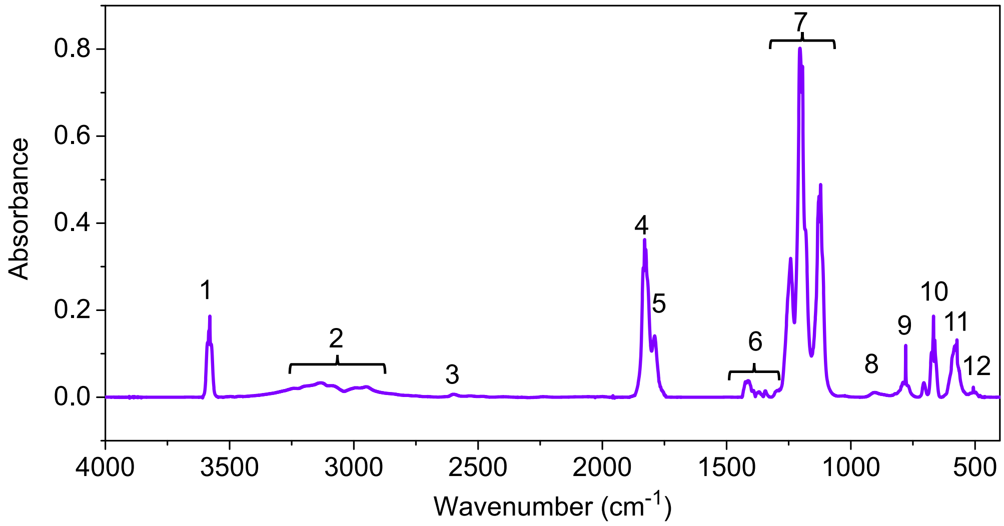

Table S3: Spectral assignment of the FTIR spectrum of pure TFA in gas phase

Band number	Frequency (cm^{-1})	Assignment
1	3579.7	ν_{OH} TFA monomer
2	3245-2950	ν_{OH} anti-symmetric TFA dimer
3	2598	ν_{OH} TFA symmetric dimer
4	1829.8	$\nu_{(C=O)}$ TFA monomer
5	1788	$\nu_{(C=O)}$ TFA dimer
6	1418-1343	($\nu_{(C—C)}$ + $\nu_{(C—O)}$ + δ_{OH} + OOP C=O) TFA monomer
7	1242-1128	δ_{OH} + $\nu_{(C—F)}$ TFA monomer
8	903	$\delta_{OH(OOP)}$ TFA dimer
9	779	γ_{OH} + OOP C(=O) TFA monomer
10	705-667	O=C—O scissoring TFA monomer
11	573	δ_{CF3} TFA monomer
12	507	($\nu_{O—H}$ + ν_{CF2}) asymmetric TFA dimer

Figure S2: Raman spectra of 7.5% w/w TFA solution in the liquid phase (a) and ice phase (b)

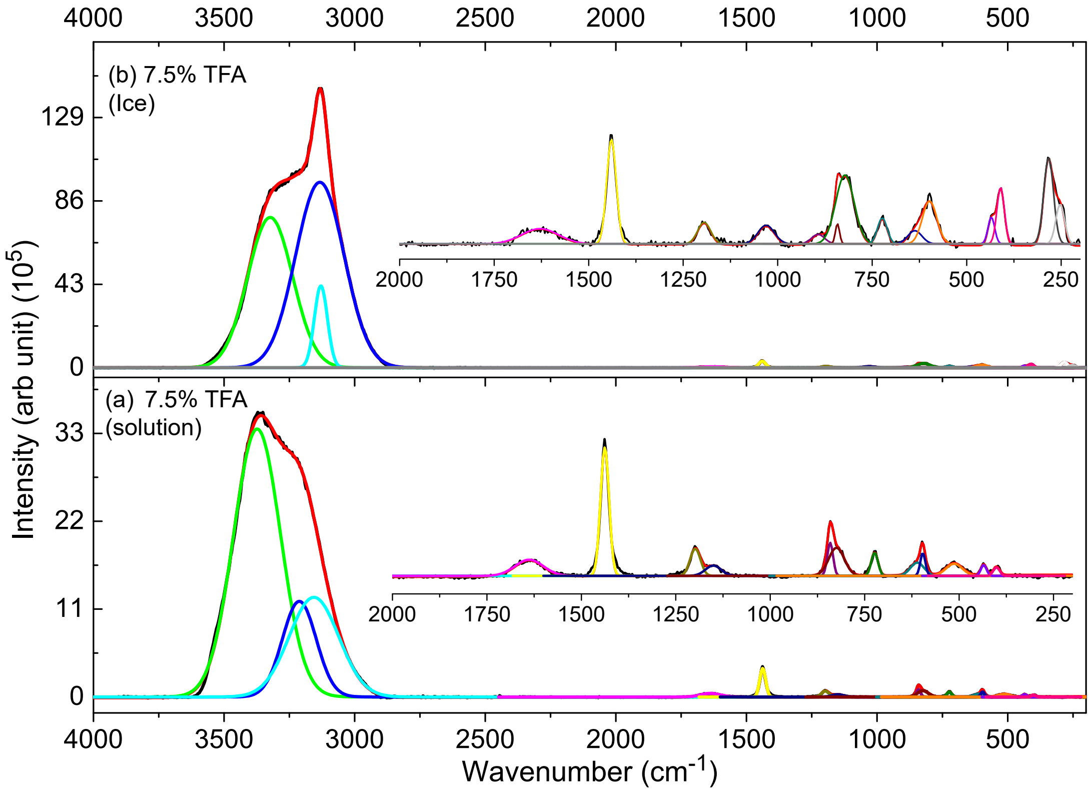

Figure S3: Raman spectra of 5% w/w TFA solution in the liquid phase (a) and ice phase (b)

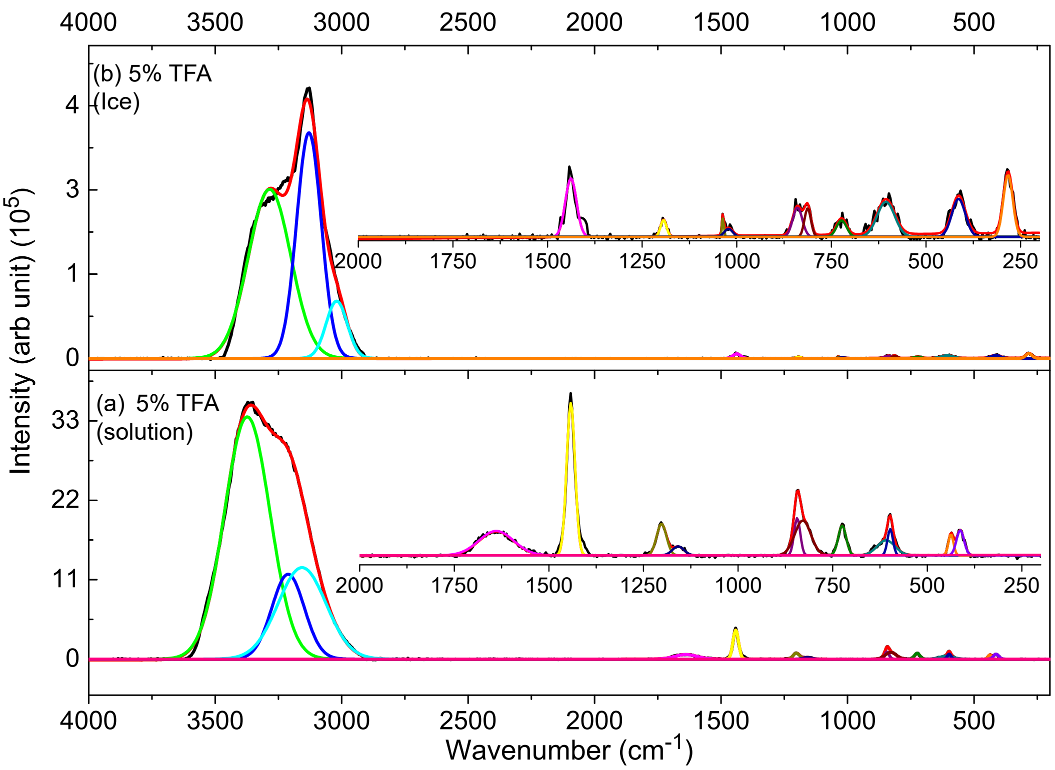

Figure S4: Raman spectra of 2.5% w/w TFA solution in the liquid phase (a) and ice phase (b)

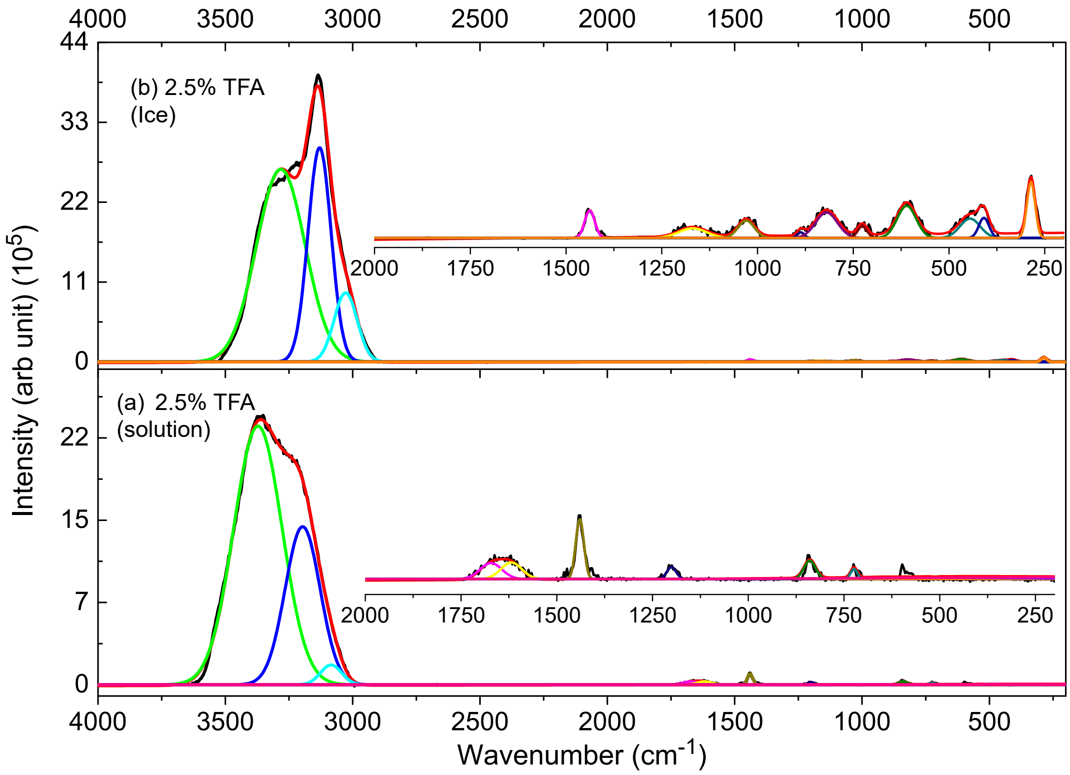

Figure S5: Raman spectra of 1% w/w TFA solution in the liquid phase (a) and ice phase (b)

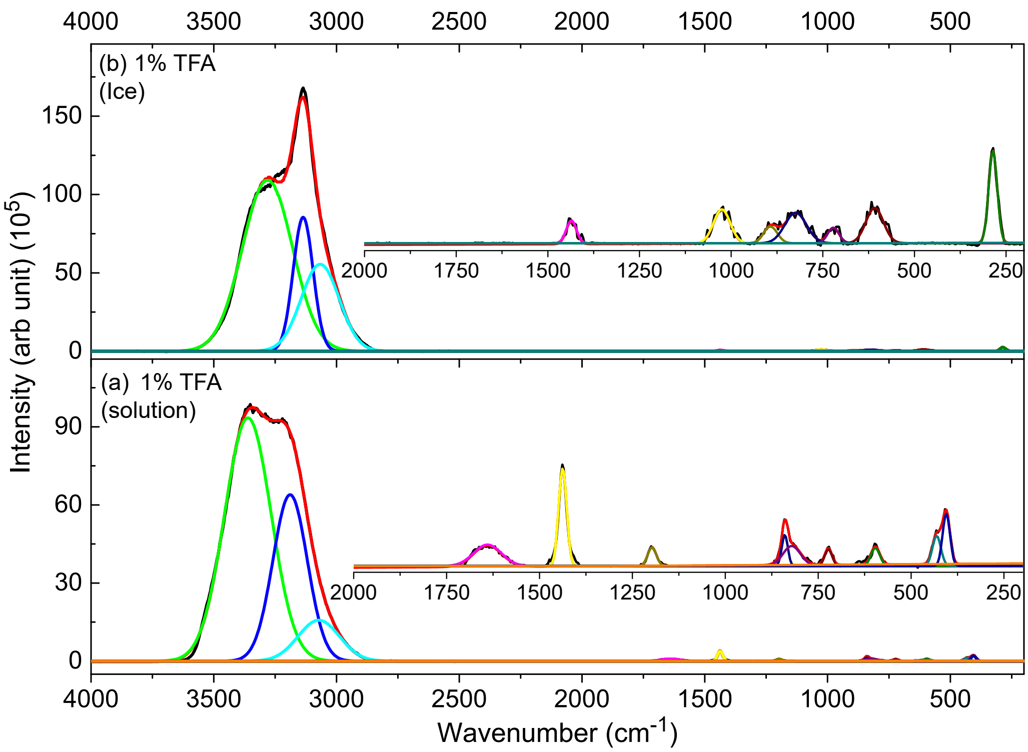

Figure S6: Depression in freezing point with the varying aqueous w/w TFA droplets

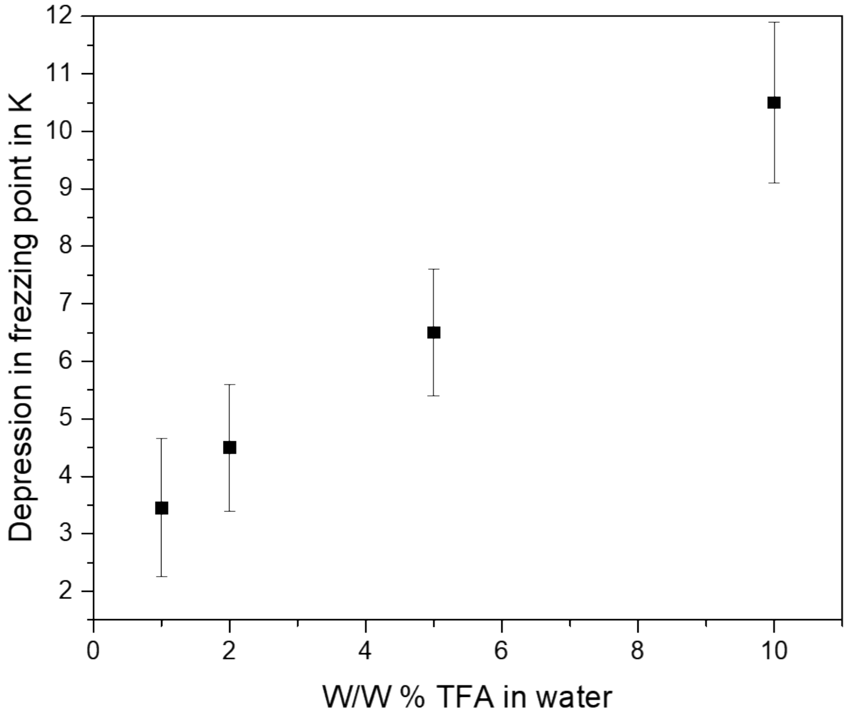

Figure S7: A representative picture of the droplet used for this study. The diameter of the droplet is (2.32 ± 0.2 mm) and the volume is (4.3 ± 0.2 μL)

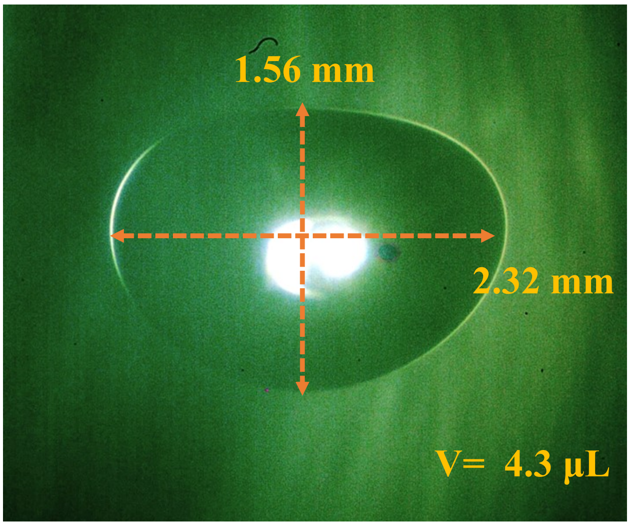

Figure S8: Representative IR image and indication of droplet freezing captured in IR camera.

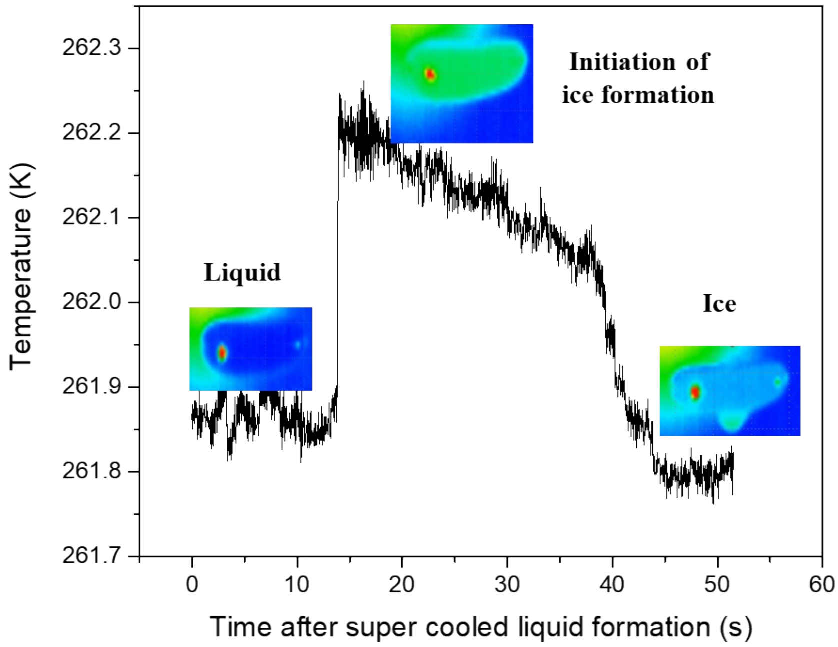

Figure S9: Distribution of atomic charge on different ice-encapsulated TFA forms (a) Dissociated TFA anion; (b) Undissociated neutral TFA.

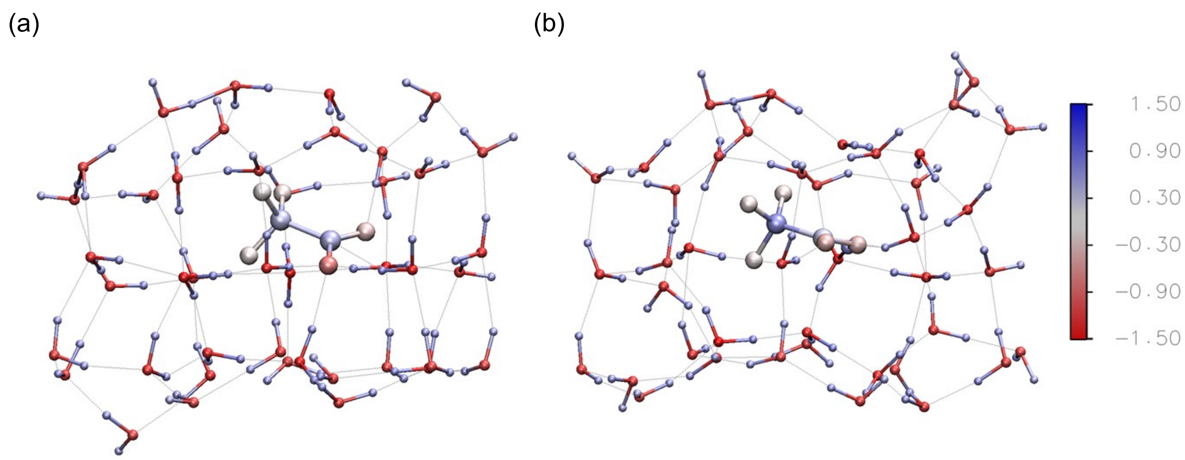

Table S4: Optimized coordinate and Mulliken charges of different ice-encapsulated TFA forms (a) Dissociated TFA anion. (b) Undissociated neutral TFA.

(a) Optimized coordinate and Mulliken charges of ice-encapsulated dissociated TFA anion :

Atom	X-coord	Y-coord	Z-coord	Mulliken
O	-2.87127258	-3.34039306	-3.26585129	-1.24
O	-1.91330534	-2.82401808	-0.65938510	-1.40
O	-4.66022419	-2.70214290	0.04669096	-1.28
O	-2.67658979	-1.94338968	4.08823833	-1.18
O	3.48504845	2.80149997	-3.01181653	-1.33
O	0.82998325	-0.87496124	-3.01045106	-1.35
O	4.94647271	-1.75415877	-3.40056773	-1.12
O	-2.61020625	1.79993874	-3.01549408	-1.25
O	-3.08561734	1.91448076	-0.24203280	-1.19
O	-0.58985876	3.03400154	-0.11973838	-1.45
O	4.38134010	1.04300219	4.42788196	-1.10
O	1.58175234	0.04269493	4.57234721	-1.34
O	4.93270968	-2.44081924	1.97018862	-1.15
O	-2.26839790	2.47252008	3.95839484	-1.17
O	5.71930671	0.74986026	-0.02355005	-1.26
O	1.45386161	-4.72670338	-3.07011410	-1.18
O	-6.17664115	-0.43095929	-3.02113068	-1.13
O	1.58698755	5.01819927	-2.71564338	-1.11
O	0.77399235	-4.21130586	2.10197328	-1.19
O	-6.06507592	0.46067730	1.98402591	-1.17
O	1.57938079	4.95171280	2.50267345	-1.17
O	0.71455136	-3.48436905	-0.57522800	-1.32
O	-4.91774760	-0.05456989	-0.54377907	-1.23
O	1.89832006	4.11606967	0.02145111	-1.38
O	-1.16859071	0.04630514	4.92463445	-1.19
O	-1.85326662	-0.88566460	-2.63276061	-1.28

O	2.39826368	2.31733331	3.09231274	-1.21
O	2.41027610	-2.23131632	3.28792656	-1.21
O	6.05903677	-0.07002924	2.71231814	-1.16
O	-1.15135547	4.40376368	2.21381526	-1.18
O	-4.39779129	2.57465318	2.21146869	-1.16
O	4.36801313	3.02201283	-0.32973009	-1.22
O	4.38081562	-1.53167878	-0.63230392	-1.36
O	0.97822641	1.80952865	-3.27315313	-1.13
O	2.43025607	-2.45618018	-4.36271788	-1.19
O	5.66264490	0.99211262	-3.17638679	-1.11
O	-1.05333514	4.15220417	-2.51072341	-1.18
O	-4.71142203	1.14287632	-4.64810812	-1.07
O	-1.79861962	-3.61634782	2.06332983	-1.25
O	-5.08863767	-1.85105080	2.66399228	-1.15
O	-1.02230243	-5.07030260	-4.40625843	-1.05
O	-5.64599799	-3.16237189	-2.70416111	-1.14
H	-2.59111339	-3.47154645	-2.33365736	0.61
H	-1.89671020	-1.93636227	-1.09631922	0.64
H	-3.74200628	-3.00254965	-0.10419143	0.61
H	-2.81648358	-2.46349750	4.89382241	0.50
H	3.65914936	2.85220812	-2.04946213	0.65
H	1.22432498	-0.91375585	-2.11680961	0.65
H	4.82104694	-1.85182629	-2.43514810	0.58
H	-3.03408763	2.01638568	-2.16073460	0.59
H	-3.47555288	2.32235467	0.55642471	0.59
H	-0.85656233	3.57800192	0.66449288	0.68
H	3.71075473	0.45149553	4.82279615	0.55
H	1.65488173	0.83272224	3.99551255	0.64
H	5.43502441	-3.22316697	2.24104634	0.51
H	-2.56622068	2.86672984	4.79228073	0.52

H	5.91671522	0.59274062	0.92286887	0.60
H	1.21498449	-4.35121625	-2.19858140	0.60
H	-5.78860909	-0.20300616	-2.14887170	0.59
H	1.72237572	4.88861755	-1.75400612	0.58
H	0.88407907	-5.11159575	2.44138530	0.51
H	-7.02076534	0.42236819	2.13674996	0.50
H	2.01811378	5.78754461	2.71715535	0.50
H	-2.62195976	-2.39202716	-3.38960175	0.61
H	-0.96474962	-3.12964304	-0.68468598	0.69
H	-4.65501032	-1.75489606	-0.24334020	0.66
H	-2.06827342	-1.18278325	4.36037076	0.63
H	2.61720568	2.33027152	-3.10278089	0.66
H	1.41714836	-1.45910511	-3.59627366	0.65
H	5.19091106	-0.80681971	-3.50211331	0.58
H	-3.34922806	1.66424884	-3.66145472	0.62
H	-2.11010326	2.06174898	-0.16368264	0.62
H	-0.82397446	3.55647692	-0.93694284	0.67
H	3.81567104	1.68120865	3.92418797	0.60
H	1.81950564	-0.74418771	4.02134991	0.66
H	5.44041947	-1.64741380	2.28045254	0.61
H	-3.07032908	2.41872626	3.38387481	0.62
H	5.19744369	-0.05311101	-0.29427526	0.66
H	0.60279095	-4.87627294	-3.53768337	0.60
H	-6.06881951	-1.41218202	-3.06619012	0.60
H	2.25046185	4.41861640	-3.11419516	0.57
H	-0.20884695	-3.99848634	2.16885844	0.64
H	-5.68190939	-0.42393595	2.31964732	0.62
H	1.76273656	4.75795328	1.53179662	0.64
H	1.09175051	-2.57812630	-0.48275074	0.67
H	2.72002241	3.57376690	-0.01510453	0.66

H	-1.44325405	0.87061850	4.47252357	0.60
H	-0.18413346	-0.01572291	4.81977992	0.65
H	-4.11384747	0.52173596	-0.51264861	0.63
H	1.12580132	3.49742378	-0.04373175	0.70
H	-2.12538687	0.05275516	-2.77279117	0.63
H	-0.88668330	-0.91628582	-2.85624088	0.67
H	2.31071200	1.95467507	2.17645566	0.60
H	3.25178654	-2.29769991	2.79392774	0.63
H	5.40912976	0.34436548	3.36560879	0.62
H	-1.38275279	3.71811058	2.87363926	0.61
H	-4.86369416	3.42410948	2.18872018	0.51
H	4.77362062	2.12534711	-0.14221946	0.66
H	3.42091186	-1.29516569	-0.58951583	0.68
H	0.90385034	0.82164404	-3.29217981	0.66
H	3.36019435	-2.23945546	-4.10472957	0.61
H	4.89791027	1.60887993	-3.26179444	0.60
H	-1.44695809	3.45801516	-3.07648010	0.58
H	-5.32533733	1.79461995	-5.01480003	0.48
H	-4.24013328	-1.82479278	3.16161207	0.61
H	-2.04645217	-2.96770713	2.76042377	0.65
H	-4.73786700	-3.29260741	-3.05748263	0.59
H	-1.70324425	-4.42092125	-4.10587445	0.60
H	5.11222721	3.62994825	-0.45108370	0.52
H	4.55481221	-2.06088028	0.17253656	0.61
H	-5.08552307	1.85620230	2.20606918	0.61
H	-0.25088873	4.71232395	2.45126175	0.61
H	1.79909901	-2.87921780	2.87693615	0.63
H	2.12781049	3.25872783	3.05165085	0.60
H	6.93709187	0.02938310	3.10936772	0.50
H	-5.27057028	0.50415689	-4.12136199	0.60

H	-0.17525403	4.42580842	-2.86877144	0.61
H	2.21948966	-3.34132830	-3.97941360	0.61
H	0.32531366	2.11410033	-2.62382034	0.53
H	5.92740569	1.03531333	-2.24193281	0.54
H	0.86484602	-3.89906233	0.30389479	0.63
H	-5.45336181	0.21868802	0.23070613	0.59
H	-1.90651926	-3.16072433	1.20133040	0.63
H	-4.90517930	-2.31474022	1.80826550	0.61
H	-1.45668953	-5.93475986	-4.38240407	0.47
H	-5.52017851	-3.19155897	-1.73450572	0.57
C	0.09720217	-0.01590353	1.08949005	0.39
C	1.52068078	0.03280702	0.44454180	0.43
F	-0.85849898	0.00406578	0.13202356	-0.18
F	-0.14267640	1.00537199	1.93595491	-0.21
F	-0.07418616	-1.16528820	1.79407939	-0.15
O	2.27355795	0.97069690	0.73574550	-0.33
O	1.74371621	-0.93850939	-0.34059155	-0.74

(b) Optimized coordinate and Mulliken charges of ice-encapsulated undissociated neutral TFA:

Atom	X-coord	Y-coord	Z-coord	Mulliken
O	-2.39662871	-1.00734716	-2.58602912	-1.52
O	-2.24917643	-4.22879495	-0.10992939	-1.31
O	-3.64966839	-1.82159801	-0.27767736	-1.16
O	-2.10498366	-2.32093752	4.21561400	-1.18
O	5.24300128	2.49190549	-3.25510616	-1.16
O	2.18397125	-0.25025756	-3.71572668	-1.24
O	4.29765421	-1.56169931	-2.59243474	-1.19
O	-3.27496398	1.64441983	-2.79400785	-1.25
O	-4.90789551	1.89804647	-0.61043458	-1.22
O	-0.00036904	3.19460550	0.06440234	-1.39

O	4.68916454	1.71178128	4.89036302	-1.08
O	1.25341517	-0.22503447	3.07194594	-1.27
O	5.33378644	-2.43603128	3.87286374	-1.05
O	-2.38051566	2.29969638	3.82761047	-1.20
O	4.62971707	0.99884261	1.10886643	-1.27
O	0.50272270	-4.36036722	-3.42645038	-1.09
O	-6.70526296	-0.55307155	-3.15240788	-1.14
O	1.26194791	4.47973425	-3.12396475	-1.14
O	1.34181887	-4.62358328	1.85629943	-1.17
O	-6.14887847	-0.55925604	2.40027235	-1.14
O	1.97557219	4.65824929	2.30615154	-1.15
O	0.41143796	-3.77280112	-0.65263894	-1.26
O	-6.08294107	-0.59301466	-0.40838842	-1.26
O	2.23287827	4.60925703	-0.45699222	-1.33
O	-0.94346758	-0.03132606	4.66941937	-1.23
O	-0.06464418	0.17994421	-2.31965387	-1.30
O	2.89051460	2.06135378	2.91127680	-1.34
O	2.92658676	-2.42481646	2.54833000	-1.24
O	6.20994128	0.17367319	3.30359590	-1.16
O	-0.89338555	4.17986373	2.33334038	-1.17
O	-4.44410555	1.72698390	2.18047675	-1.14
O	4.60623016	3.15500609	-0.52511749	-1.18
O	3.71176002	-1.33459622	0.15571295	-1.28
O	2.77847218	2.35398471	-4.45057865	-1.16
O	2.39365072	-2.75279505	-4.67985806	-1.13
O	6.42855758	0.05797485	-3.19738215	-1.09
O	-0.89819225	2.85789132	-2.39552339	-1.17
O	-5.93259429	1.98571814	-3.32450679	-1.14
O	-1.23196622	-4.41621408	2.50898043	-1.19
O	-4.13540699	-2.34168259	2.47250874	-1.22

O	-2.34139406	-3.82611157	-3.18827944	-1.21
O	-4.54241361	-1.94341386	-4.16510886	-1.04
H	-2.70616211	-1.15373401	-1.66172443	0.68
H	-2.77249062	-3.40825010	-0.23636066	0.66
H	-3.53935487	-1.66485120	0.68083922	0.58
H	-2.22241152	-2.71152694	5.09499737	0.52
H	4.97614942	2.68551375	-2.33551063	0.59
H	2.95479978	-0.54416066	-3.16510984	0.63
H	4.29598870	-1.66293759	-1.61928601	0.57
H	-3.02763563	0.69070327	-2.86556201	0.64
H	-4.13301825	1.77853764	-1.21553864	0.62
H	-0.50621866	3.55671671	0.85208728	0.66
H	4.25799007	1.29646859	5.65223993	0.50
H	1.81141131	0.58122490	3.03570331	0.66
H	5.54762860	-2.62318352	4.79807606	0.48
H	-2.84024434	2.74645901	4.55517212	0.53
H	5.33846360	0.71126373	1.72579601	0.60
H	0.58666792	-4.22663022	-2.46001026	0.58
H	-6.70183614	-0.75269685	-2.19429796	0.58
H	1.68711627	4.69615730	-2.25967909	0.58
H	1.62570688	-5.53754490	2.01036326	0.51
H	-6.83669047	-0.63211297	3.07859558	0.51
H	2.41116287	5.37849003	2.78695144	0.52
H	-1.45789218	-0.65119766	-2.53007856	0.69
H	-1.32128517	-4.02366905	-0.38408111	0.66
H	-4.58507187	-1.54604505	-0.45084664	0.63
H	-1.66993034	-1.41287544	4.36824523	0.63
H	4.39293141	2.46821871	-3.76572580	0.61
H	2.06660053	-1.05512030	-4.28943409	0.60
H	5.11898584	-1.05568805	-2.81590034	0.60

H	-4.12927325	1.76785056	-3.27258459	0.63
H	-5.54939026	2.35408641	-1.18784758	0.57
H	-0.56382305	3.14238455	-0.75222657	0.66
H	3.96179698	1.92321711	4.24403491	0.62
H	1.85012582	-1.00087008	2.96525718	0.64
H	5.71256913	-1.54977467	3.67090695	0.59
H	-3.09886057	2.05838472	3.17842377	0.63
H	4.28635936	0.15786851	0.68581108	0.67
H	-0.45641615	-4.25849896	-3.59497543	0.57
H	-6.02400672	-1.14560904	-3.55278249	0.60
H	1.47754727	5.20835077	-3.72586352	0.52
H	0.39422216	-4.56098571	2.18865479	0.62
H	-5.49405646	-1.28773811	2.55835211	0.60
H	2.12412497	4.83578504	1.34023710	0.59
H	0.55502933	-2.81942767	-0.48714607	0.64
H	3.02468687	4.02193023	-0.51235765	0.67
H	-1.43133023	0.75825603	4.34886822	0.61
H	-0.10590657	-0.07466769	4.14200988	0.65
H	-5.68011198	0.30936139	-0.46898876	0.65
H	1.43932759	4.03111991	-0.32576129	0.67
H	-0.22750466	1.13794570	-2.44795274	0.62
H	0.76796519	-0.03404600	-2.82295491	0.68
H	3.44071947	1.74385161	2.14884718	0.68
H	3.69790816	-2.60519604	3.13310738	0.60
H	5.73768821	0.74819695	3.97191562	0.61
H	-1.32025947	3.51771775	2.92363833	0.63
H	-4.53568443	1.96018276	1.23259128	0.60
H	4.69564095	2.33898620	0.03681495	0.64
H	2.77212917	-1.17824738	-0.08418528	0.61
H	2.49898123	1.42097156	-4.29031867	0.61

H	3.16020207	-2.82614897	-4.08266855	0.54
H	6.02556718	0.96821716	-3.26328356	0.61
H	-1.79939401	2.66407453	-2.74703395	0.60
H	-6.39450187	2.43925664	-4.04521455	0.51
H	-3.43087558	-2.29899340	3.17591828	0.64
H	-1.42785290	-3.60832874	3.02857229	0.61
H	-3.75526048	-1.52042207	-3.76692469	0.58
H	-2.22299443	-2.88418174	-2.94216644	0.63
H	5.37152280	3.71260754	-0.31629984	0.52
H	3.60771253	-1.86427959	0.98442122	0.63
H	-5.05262818	0.97390430	2.32714479	0.60
H	0.01075137	4.35119262	2.65976447	0.59
H	2.43006253	-3.26337712	2.39927877	0.60
H	2.56013240	2.96032882	2.68674824	0.64
H	7.15425887	0.38532048	3.36177980	0.51
H	-6.28066703	1.04041424	-3.31486518	0.60
H	-0.42361080	3.51798676	-2.94007163	0.57
H	1.70467117	-3.35471957	-4.30505158	0.61
H	2.16461984	2.93129407	-3.95907644	0.58
H	6.87314209	-0.09924093	-4.04321403	0.48
H	0.87179506	-4.21002960	0.09843341	0.61
H	-6.40498755	-0.65708395	0.51476788	0.59
H	-1.70047524	-4.33696815	1.64188501	0.61
H	-4.23156083	-3.27927039	2.24137004	0.54
H	-2.49074386	-4.29310580	-2.34556708	0.56
H	-4.31647886	-2.88977759	-4.15438385	0.52
C	-0.90818640	0.12510379	0.88935929	0.63
C	0.55086207	-0.06583768	0.37313587	0.29
F	-1.38651546	-1.02625070	1.39096498	-0.20
F	-1.73390408	0.52413781	-0.10375638	-0.17

F	-0.96940054	1.06598482	1.84923642	-0.21
O	1.26566681	1.01192197	0.24118365	-0.40
O	0.96845506	-1.18623245	0.14447335	-0.44
H	0.71412554	1.87904844	0.27500761	0.65

Figure S10

(i): Optimized deprotonated $TFA^-/(H_2O)n$ clusters with amorphous water. The number of water molecules n in the clusters are (a) zero, (b)one, (c) two, (d) three, (e) four, (f) five, (g) six, (h) seven, (i) eight, (j) nine, (k) ten, (l) twelve, (m) fourteen, (n) sixteen, (o) eighteen, and (p) twenty. The atoms in the water molecules are represented using smaller spheres to aid visualization. Hydrogen bonds are denoted with red dashed lines.

(ii): Optimized neutral $TFA^0/(H_2O)n$ clusters with amorphous water. The number of water molecules n in the clusters are (a) zero, (b)one, (c) two, (d) three, (e) four, (f) five, (g) six, (h) seven, (i) eight, (j) nine, (k) ten, (l) twelve, (m) fourteen, (n) sixteen, (o) eighteen, and (p) twenty. The atoms in the water molecules are represented using smaller spheres to aid visualization. Hydrogen bonds are denoted with red dashed lines. Gray boxes represent clusters which were found to form hydronium by deprotonating TFA during optimization.

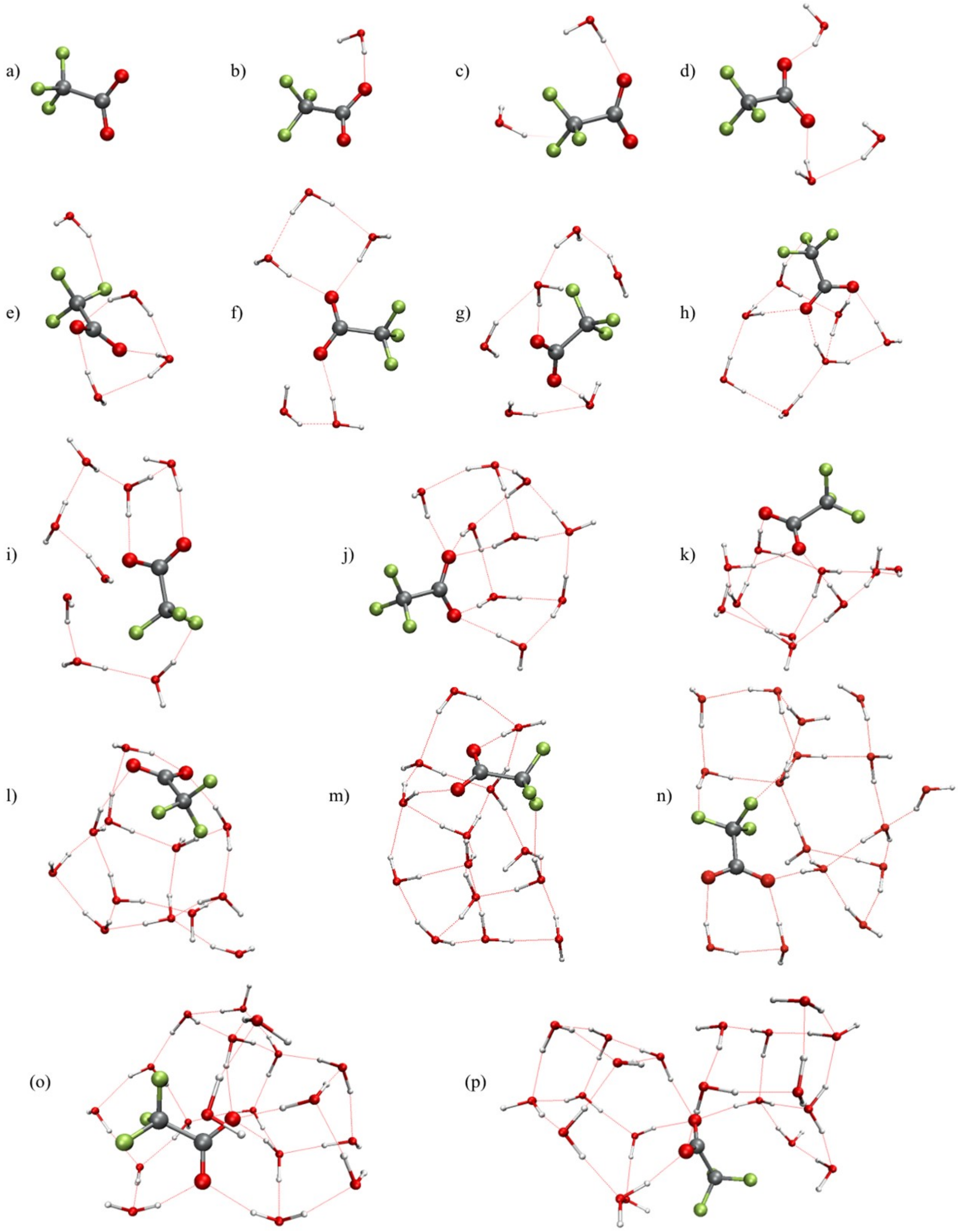
a)
b)
c)
d)
e)
f)
g)
h)
i)
j)
k)
l)
m)
n)
(o)
(p)

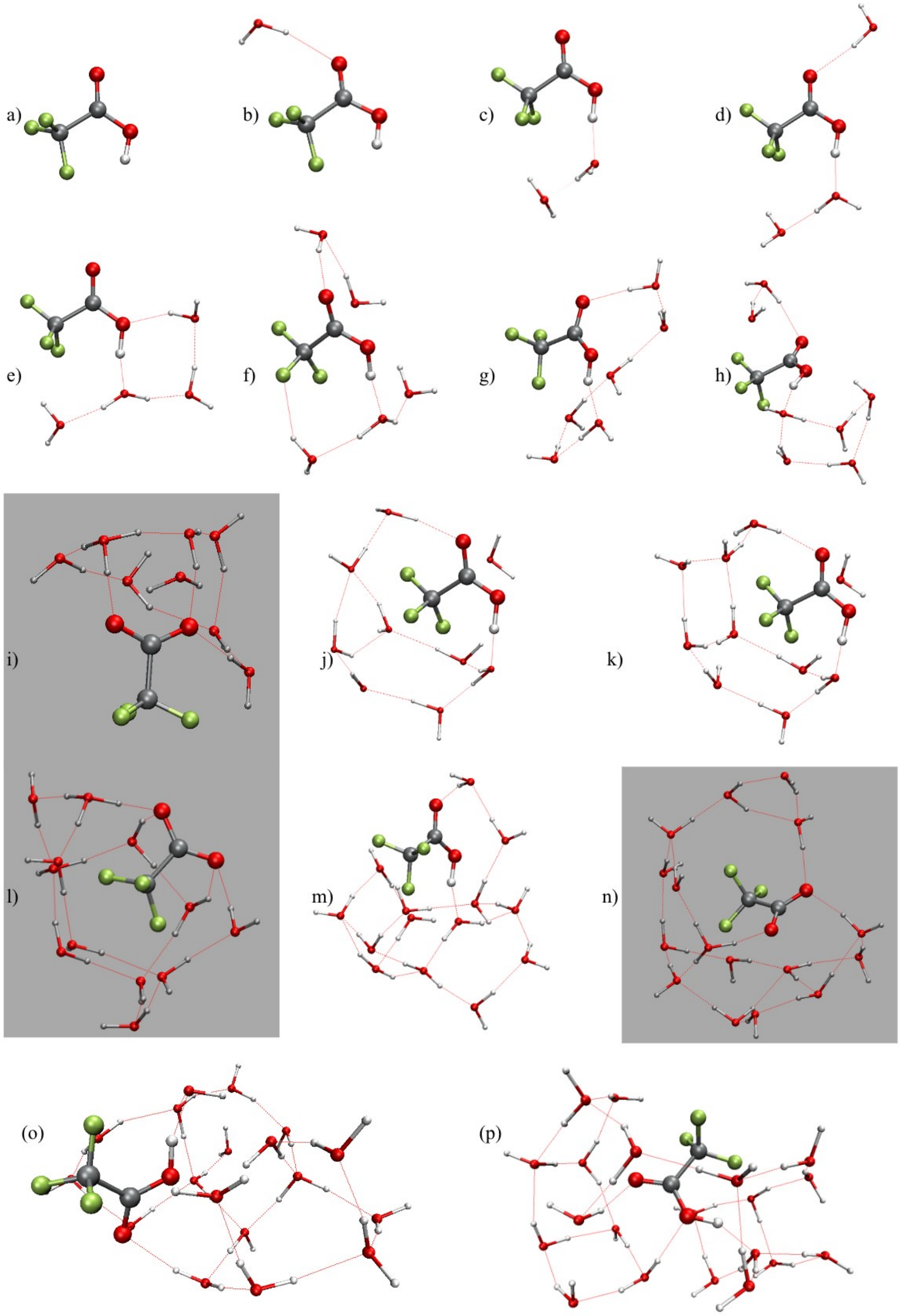
a)
b)
c)
d)
e)
f)
g)
h)
i)
j)
k)
l)
m)
n)
(o)
(p)